

Methodology and Geophysical Data

- 3.1 Introduction
- 3.2 Gravity Measurements at Sea
- 3.3 Gravity Anomaly Computation
 - 3.3.1 The Latitude Correction
 - 3.3.2 The Free-air Correction and Free-air Gravity Anomaly
 - 3.3.3 The Eötvös correction
- 3.4 Interpretation of Gravity Anomaly using Two-dimensional Gravity Forward Modeling
- 3.5 Theoretical Basis of Isostatic Compensation
 - 3.5.1 Isostatic Response Functions
 - 3.5.2 The Gravitational Admittance
 - 3.5.3 Gravitational Admittance and Isostatic Models
- 3.6 Computation of Admittance from Observed Data
- 3.7 Process Oriented Gravity Modeling
- 3.8 Geophysical Data

Methodology and Geophysical Data

3.1 Introduction

Gravitation is the attractive force existing between any two objects that have mass in the universe. According to Newton's law of universal gravitation the magnitude of this force between two bodies of masses m_1 and m_2 kilograms separated by a distance r meter is given by

$$F = \frac{Gm_1m_2}{r^2} \quad \dots (3.1)$$

Where, G is the universal constant of gravitation ($6.7 \times 10^{-11} \text{ Nm}^2/\text{kg}^2$). In Geophysics, the gravitational acceleration (g) - the gravitational force per unit mass- is often considered more important than the absolute magnitude of the force. If the planet Earth were a non-rotating spherically symmetrical body, the gravitational acceleration on its surface would remain constant. The Earth behaves as an elastic body and deforms in response to the forces generated by its rotation, therefore it becomes slightly flattened at the poles and with a compensating bulge at the equator. The equatorial bulge and the effects of centrifugal force together cause an increase in mean that sea-level gravitational acceleration of about 0.5% from equator to poles.

The figure of the Earth is the shape of an equipotential surface of gravity, in particular the one that coincides with mean sea level, which is called geoid (Li and Götze, 2001). The best mathematical approximation to the shape of the Earth is an oblate ellipsoid, or spheroid. In 1980, the International Association of Geodesy adopted the Geodetic Reference System (GRS 80) in which the International Reference Ellipsoid or the Normal Earth has an equatorial radius (a) equal to 6378.137 km and a polar radius (c) equal to 6356.752 km (Moritz, 1980).

The gravity field due to this equipotential ellipsoid of revolution is referred as theoretical or normal gravity. The normal gravity field at any point on the Earth's surface can be computed using the International Gravity Formula (IGF) as given below (Moritz, 1980)

$$g_n = g_e (1 + \beta_1 \sin^2 \phi + \beta_2 \sin^2 2\phi) \quad \dots (3.2)$$

The constants in the formula for GRS80, are: $g_e = 9.780327 \text{ ms}^{-2}$; $\beta_1 = 5.302441 \times 10^{-3}$; $\beta_2 = -5.810 \times 10^{-6}$. They are used in calculation of normal gravity at any latitude with an accuracy of 0.1 mGal.

3.2 Gravity Measurements at Sea

The gravity measurements at sea surface are severely effected by the vertical and horizontal accelerations generated by the wave action of sea water and movement of the ship/ boat corresponding to sea conditions. The ship's vertical and horizontal accelerations are compensated by mounting the gravimeter sensors on gimbals or stabilized platforms. The Vening-Meinesz pendulum is the earliest instrument that has measured gravity at sea to an accuracy of 5-15 mGal on board submarines, which could handle small and long period accelerations (Telford et al., 1990). The Graf Askania gravimeters mounted on elaborate gyro-stabilized platform have been successful in measuring gravity readings onboard surface-ships with an accuracy of 2 mGal. The new Lacoste-Romberg gravity meters which are being routinely used onboard research vessels have good accuracies of ~1 mGal.

3.3 Gravity Anomaly Computation

The reduction of the gravity data acquired at sea requires knowledge of absolute gravity field at the location generally referred as a base station value. This is the location where the ship/ boat is berthed prior to the start of data acquisition. The measured values are tied to this base station value in order to calculate the gravity values along the traverse. The gravity values, thus computed must be corrected for latitude, elevation and topography in order to obtain the gravity values corresponding to some datum like geoid or ellipsoid. In addition the corrections for instrumental drift, Earth tide and the motion of ship are also necessary to carry out. A short description of important gravity correction applied for marine gravity measurements is given below.

3.3.1 The Latitude Correction

The theoretical gravity at given latitude position is calculated by the normal gravity formula (Eq. 3.2). If the measured gravity is an absolute value, then the latitude correction is made by subtracting the value calculated using the normal gravity formula. Gravity surveys are often carried out with a gravimeter, which measures the gravity difference relative to a base station. Therefore, the normal reference gravity g_n may then be replaced by a latitude correction, obtained by differentiating Eq. (3.2) (Telford et al., 1990)

$$\Delta g_L / \Delta s = \left(\frac{1}{R_e} \right) \frac{\Delta g}{\Delta \phi} \quad \dots (3.3)$$

Where, $\Delta s = R_e \Delta \phi$ is the N-S distance and R_e is the radius of Earth (6368 km). Therefore Eq.3.3 becomes

$$\Delta g_L / \Delta s \approx 0.811 \sin 2\phi \quad mGal/km \quad \dots (3.4)$$

This correction is zero at poles and equator and maximum at 45° .

3.3.2 The Free-air Correction and Free-air Gravity Anomaly

The Free-air correction accounts for the height of the gravity station above the ellipsoid 'h'. The free-air correction is given by the second approximation of international 1924 ellipsoid (Moritz, 1980)

$$\partial g_{FC} = -(0.30877 - .00045 \sin^2 \phi)h + 0.000072h^2 \quad \dots (3.5)$$

Ignoring the second order term and setting $\phi = 45^\circ$, the first approximation of the height correction is

$$\partial g_{FC} = -0.30877h \quad mGal \quad \dots (3.6)$$

Thus, the free-air correction formula suggests that for every 1 m change in height, the gravity value changes by a factor of 0.30877 mGal. Free-air correction is positive for the gravity stations lie above the datum plane and negative for stations lie below the datum. In general, elevation or height above the geoid is used rather than ellipsoidal height for computing the free-air correction. The gravity anomaly derived after applying free-air correction is known as free-air anomaly and is expresses as

$$F.A.A = (g_{obs} - g_{ellipsoid}) \pm \partial g_{FC} \quad \dots (3.7)$$

Where, g_{obs} and $g_{ellipsoid}$ are observed and ellipsoidal gravity respectively. Marine gravity measurements are done at mean sea level; hence no free-air correction is required to be considered. The small changes caused by sea surface elevations due to tides are generally ignored (Nettleton, 1976).

3.3.3 The Eótvós Correction

During the marine gravity surveys, the motion of research vessel generates additional centrifugal force which affects the gravity measurements. An eastward component of velocity adds to the rotation of the Earth and causes slight increase in the centrifugal force and thus causes a reduction in measured gravity, whereas the westward component has the opposite effect. The Eótvós correction for a ship moving with a velocity V heading at angle θ from true north at a latitude ϕ is given by (Telford et al., 1990)

$$\partial g_{eotvos} = 4.04V \cos \phi \sin \theta + 0.0012V^2 \text{ mGal} \quad \dots (3.8)$$

3.4 Interpretation of Gravity Anomaly using Two-Dimensional Gravity Forward Modeling

The gravity anomalies after applying corrections, in general, represent density inhomogeneities within the Earth. The simple way to interpret these anomalies is by forward modeling, which involves computation of gravity effect of assumed causative bodies and compare with observed anomalies. For bodies of regular geometry, forward modeling is carried out using standard anomaly equations. Models of arbitrary shape are, in principle, divided into several bodies of regular shape and then their individual gravity contributions are calculated and added. In a classic paper, Talwani et al., (1959) presented a method to compute the gravity effect of any two-dimensional body of arbitrary shape by approximating it to an n -sided polygon. The polygons are defined in terms of coordinates of vertices and the gravity anomaly is computed using line integral method.

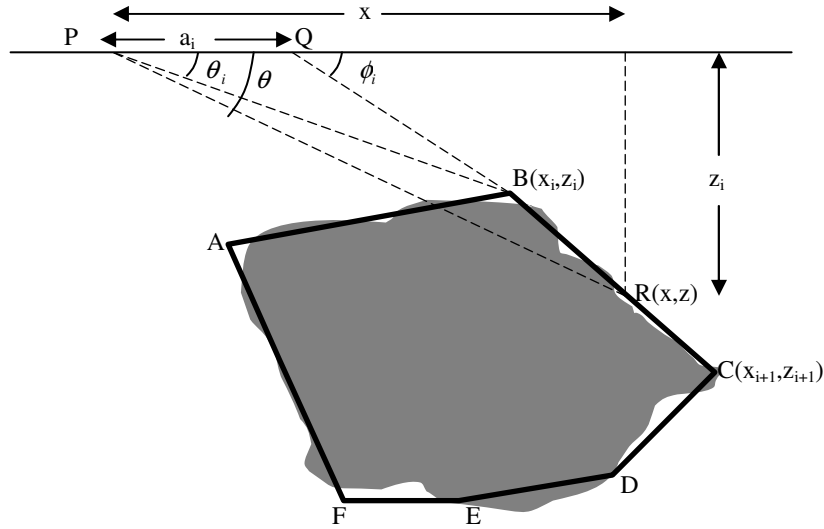


Figure 3.1 Polygon approximation of irregular vertical section of two-dimensional body. Geometrical elements involved in the gravity computation are depicted.

The polygon ABCDEF approximates an arbitrary shaped body (Figure 3.1). The gravity effect of the polygon at the observation point P is given by (Hubbert, 1948)

$$g = 2G\rho z d\theta \quad \dots (3.9)$$

Where, G is the universal gravitational constant and ρ is the volume density. From geometry (Figure (3.1) it follows that

$$z = x \tan \theta = (x - a_i) \tan \phi_i = \frac{(a_i \tan \theta \tan \phi_i)}{(\tan \phi_i - \tan \theta)} \quad \dots (3.10)$$

The line integral for the side BC is given by

$$\int_{BC} z d\theta = \int_B^C \frac{(a_i \tan \theta \tan \phi_i)}{(\tan \phi_i - \tan \theta)} d\theta = Z_i \quad \dots (3.11)$$

Thus, for an n sided polygon Eq. 3.11 can be written as

$$g = 2G\rho \sum_{i=1}^n Z_i \quad \dots (3.12)$$

The general solution of the above equation is

$$Z_i = a_i \sin \phi_i \cos \phi_i \left[(\theta_i - \theta_{i+1}) + \tan \phi_i \cdot \log \left\{ \frac{\cos \theta_i (\tan \theta_i - \tan \phi_i)}{\cos \theta_{i+1} (\tan \theta_{i+1} - \tan \phi_i)} \right\} \right] \quad \dots (3.13)$$

Where, $\theta_i = \tan^{-1}\left(\frac{Z_i}{x_i}\right)$, $\phi_i = \tan^{-1}\left(\frac{Z_{i+1}-Z_i}{x_{i+1}-x_i}\right)$ and $a_i = x_{i+1} - Z_{i+1} \cot \phi_i$

The gravity forward model studies described in chapters 4, 5, and 6 have been carried out using the above method as implemented in the GM-SYS software.

3.5 Theoretical Basis of Isostatic Compensation

The isostasy of geological features is modeled by applying the theory of bending elastic plate in response to applied forces. The response of a thin, continuous, homogeneous elastic plate floating on a fluid mantle that is subjected to a line load can be represented with the following differential equation (McKenzie and Bowin, 1976; Watts, 2001)

$$D \frac{dy^4}{dx^4} + (p - q) = 0 \quad \dots (3.14)$$

where, q is the downward pressure, p is the restoring upward force, y is the deflection produced, g is the acceleration due to gravity and D is the flexural rigidity of the plate. The flexural rigidity depends on the Young's modulus E , and Poisson's ratio ν of the plate and could be expressed as

$$D = \frac{ETe^3}{12(1-\nu^2)} \quad \dots (3.15)$$

Where, Te is the approximate thickness of Earth's uppermost, elastically deforming elastic layer and commonly referred as effective elastic thickness or elastic plate thickness.

If we consider that the depression produced by the bending of plate is filled by crustal rocks of density ρ_c , and it displaces mantle of density ρ_m , then the force terms p and q in the Eq. (3.14) could be expressed as

$$q = \rho_c y g \quad \dots (3.16)$$

$$p = \rho_m y g \quad \dots (3.17)$$

Substituting Eq. 3.16 and Eq.3.17 on Eq. 3.14

$$D \frac{dy^4}{dx^4} + (\rho_m - \rho_c) y g = 0 \quad \dots (3.18)$$

3.5.1 Isostatic Response Functions

Elastic plate theory suggests that the lithosphere does not respond locally to long-term geological loads, as the Airy and Pratt models would predict. The compensation takes place regionally by a flexure over a wide region. Thereby the lithosphere behaves like a

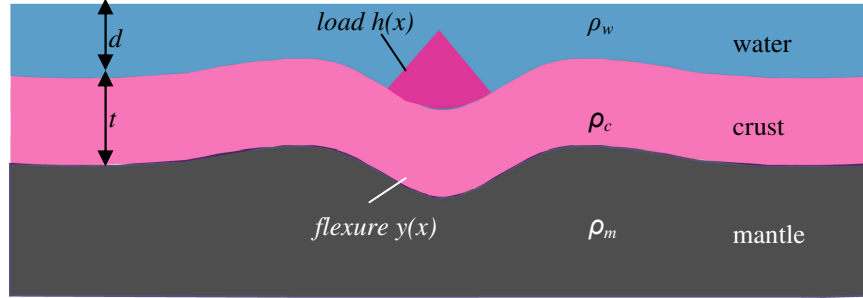


Figure 3.2 Elastic plate approximation of the bending oceanic lithosphere under load.

linear space-invariant filter that suppress the short-wavelength and high amplitude deformation associated with local models of isostasy and passes the long-wavelength deformation (small amplitude) corresponding to the flexural behavior of the lithospheric plate (Watts, 2001). Therefore, if the input load is periodic, then the output flexure is also periodic. The elastic response of a plate to a periodic load (Figure 3.2) is given for one dimension by (Watts, 2001)

$$D \frac{dy^4}{dx^4} + (\rho_m - \rho_c) y g = (\rho_c - \rho_w) g h \cos(kx) \quad \dots (3.19)$$

Where h is the amplitude of the load, k is the wavenumber of the load along x direction.

The solution of Eq.19 is periodic and of the form

$$y = \frac{(\rho_c - \rho_w) h \cos(kx)}{(\rho_m - \rho_c)} \left[1 + \frac{Dk^4}{g(\rho_m - \rho_c)} \right]^{-1} \quad \dots(3.20)$$

Let us consider that the plate is extremely weak, i.e. $D \rightarrow 0$, then $y \rightarrow \frac{(\rho_c - \rho_w)h \cos(kx)}{(\rho_m - \rho_c)}$,

this is Airy isostatic response to the periodic loading. If we assume that the plate is of enormous strength, i.e. $D \rightarrow \infty$, then $y \rightarrow 0$ which is the Bouguer isostatic response. If the plate has a finite strength, then it responds by flexure.

The wavenumber parameter which modifies the Airy response to give flexure is known as Isostatic Response Function ($\Phi_e(k)$).

$$\Phi_e(k) = \left[1 + \frac{Dk^4}{g(\rho_m - \rho_c)} \right]^{-1} \quad \dots (3.21)$$

For low wavenumber loads ($k \rightarrow 0$), the plate behaves as a weak body and deforms with Airy response, whereas for high-wavenumber loads ($k \rightarrow \infty$), the plate becomes rigid. For intermediate wavenumbers ($0.001 < k < 0.1$), the response is flexural and is called diagnostic waveband for flexure.

Eq. 3.20 yields only the flexural response to a load at a particular wavenumber. However, using Fourier analysis, the load can be split into its individual spectral components to compute the response to any arbitrarily shaped load.

$$Y(k) = \frac{-(\rho_c - \rho_w)}{(\rho_m - \rho_c)} H(k) \Phi_e(k) \quad \dots (3.22)$$

where, $H(k)$ and $Y(k)$ are wavenumber domain representation of the load, $h \cos(kx)$ and the flexure ($y(x)$).

3.5.2 The Gravitational Admittance

The state of isostasy or the lithospheric flexure beneath the geological features is not always directly observable. Gravity anomalies are sensitive to both magnitude of load and flexure and act as proxies of the flexural response of the lithosphere to geological loads. As in the case of flexural studies, Fourier transform method provides an efficient way to

compute the gravity anomalies. The gravity anomaly at a point p caused by an undulating density interface is calculated as (Parker, 1972)

$$\Delta g_p(k) = e^{-kp} 2\pi G \rho \Delta H(k) \quad \dots (3.23)$$

Where, $\Delta g_p(k)$ is the Fourier Transforms of gravity anomaly, $\Delta H(k)$ is the Fourier Transforms of the undulating surface with a uniform density contrast ρ and G is the universal gravitational constant. Gravitational Admittance, the wavenumber parameter which modifies the topography to produce gravity may be expressed as

$$Z(k) = \frac{\Delta g(k)}{\Delta H(k)} \quad \dots (3.24)$$

3.5.3 Gravitational Admittance and Isostatic Models

The gravitational admittance is an important parameter as it can be used to infer the state of isostasy of geological loads. The formulation of admittance function for sea-floor topography in three different isostatic cases (Watts, 2001) is given below

Case-1: uncompensated topography

The gravitational effect of the topography at sea-floor ($\Delta g(k)_{topo}$) could be expressed as

$$\Delta g(k)_{topo} = 2\pi G (\rho_c - \rho_w) e^{-kd} H(k) \quad \dots (3.25)$$

and the admittance due to uncompensated topography ($Z(k)_{uncomp}$) is given by

$$Z(k)_{uncomp} = 2\pi G (\rho_c - \rho_w) e^{-kd} \quad \dots (3.26)$$

Where d is the average water depth

Case-2: Airy model

For Airy model, the isostatic compensation of topographic highs and lows are obtained by forming “roots” and “anti-roots” in the mantle. Hence, the gravity anomaly is the sum of two effects: one from topography ($\Delta g(k)_{topo}$) and the other from compensation ($\Delta g(k)_{comp}$)

$$\Delta g(k)_{total} = \Delta g(k)_{topo} + \Delta g(k)_{comp} \quad \dots (3.27)$$

Where the gravity effect of compensation ($\Delta g(k)_{comp}$) can be expressed as

$$\Delta g(k)_{comp} = 2\pi G(\rho_c - \rho_w) e^{-k(d+t)} R(k) \quad \dots (3.28)$$

Where t is the oceanic crust thickness and $R(k)$, the Fourier transform of the root $r(x)$ is expressed as $R(k) = -H(k) \frac{(\rho_c - \rho_w)}{(\rho_m - \rho_c)}$

$$\Delta g(k)_{total} = 2\pi G(\rho_c - \rho_w) e^{-kd} (1 - e^{-kt}) H(k) \quad \dots (3.29)$$

The admittance function is given by

$$Z(k)_{airy} = 2\pi G(\rho_c - \rho_w) e^{-kd} (1 - e^{-kt}) \quad \dots (3.30)$$

Case3: Elastic plate (flexure) model

Flexural isostasy assumes a definite strength for the lithosphere and the compensation is distributed over broader region. The gravity effect of the flexure ($\Delta g(k)_{flex}$) is computed as

$$\Delta g(k)_{flex} = 2\pi G(\rho_c - \rho_w) e^{-k(d+t)} Y(k) \quad \dots (3.31)$$

The total gravity anomaly due to flexure and topography ($\Delta g(k)_{total}$) could be expressed as

$$\Delta g(k)_{total} = 2\pi G(\rho_c - \rho_w) e^{-kd} (1 - \phi_e(k) e^{-kt}) H(k) \quad \dots (3.32)$$

The admittance function is given by

$$Z(k)_{flex1} = 2\pi G(\rho_c - \rho_w) e^{-kd} (1 - \phi_e(k) e^{-kt}) \quad \dots (3.33)$$

The above formulation considers constant densities for the load, infill material and the oceanic crust is single layered. If the load of density ρ_l is emplaced on a two layered crust with densities ρ_2 , ρ_3 and thicknesses t_2 , t_3 where the infill material has a density ρ_i (Figure 3.3), then the admittance equation becomes

$$Z(k)_{flex2} = 2\pi G(\rho_l - \rho_w) e^{-kd} \left\{ 1 - \phi_e(k) \left[\frac{(\rho_2 - \rho_i) + (\rho_3 - \rho_2) e^{-kt_2} + (\rho_m - \rho_3) e^{-k(t_2+t_3)}}{(\rho_m - \rho_i)} \right] \right\} \quad \dots (3.34)$$

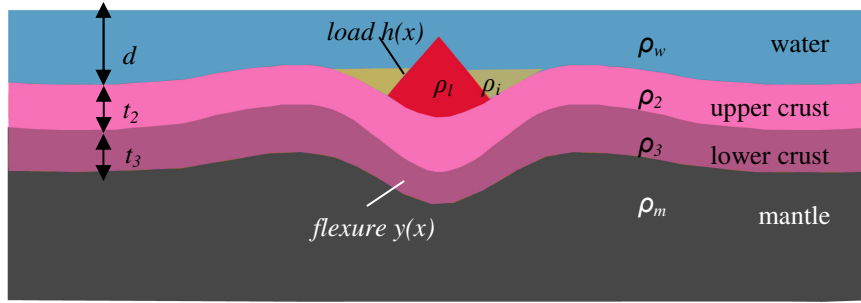


Figure 3.3 Elastic plate model for layered oceanic crust.

Case 4: flexure with subsurface load

Elastic plate model with surface and subsurface loads can provide information on underplating or presence of high density volcanic material beneath volcanic ridges and seamounts. Following McAdoo and Sandwell (1989) hypothesis, the admittance for the subsurface or buried load having a density ρ_b at a depth z below the mean depth z could be expressed as

$$Z_{buried}(k) = Z_0(k) \left[1 + \left(\frac{\rho_m - \rho_b}{\rho_b - \rho_w} \right) e^{-kh} - \left(\xi(k) \frac{\rho_m - \rho_w}{\rho_b - \rho_w} \right) e^{-kz} \right] \quad \dots (3.35)$$

Where

$$\xi(k) = 1 + \frac{Dk^4}{g(\rho_m - \rho_w)}, \quad Z_0(k) = 2\pi G(\rho_2 - \rho_w)e^{-kd}, \quad \text{and } h \text{ is the average crustal thickness}$$

Following Equation 3.34, the expression for admittance in the case of surface load for $\rho_l = \rho_i = \rho_2$ is

$$Z(k)_{surface} = 2\pi G(\rho_2 - \rho_w)e^{-kd} \left\{ 1 - \phi_e(k) \left[\frac{(\rho_3 - \rho_2)e^{-kt_2} + (\rho_m - \rho_3)e^{-k(t_2+t_3)}}{(\rho_m - \rho_2)} \right] \right\} \quad \dots (3.36)$$

The equation for combined loading: subsurface and surface can be expressed as

$$Z_{combined}(k) = \frac{\beta^2 Z_{buried}(k) + Z_{surface}(k)}{\beta^2 + 1} \quad \dots (3.37)$$

$$\text{Where, } \beta = f \left[\frac{\rho_3 - \rho_w}{\rho_m - \rho_3 + Dk^4/g} \right]$$

Where, f is the subsurface to surface load ratio

3.6 Computation of Admittance from Observed Data

Admittance analysis investigates the relationship between bathymetry and gravity anomaly in the discrete Fourier transform domain (McKenzie and Bowin, 1976; Watts, 1978). This essentially involves computation of admittance function from the observed bathymetry and gravity data and compare with the theoretical admittance to derive isostatic parameters, such as T_e , t , d and ρ_c . The admittance between gravity and bathymetry data can be calculated as suggested by McKenzie and Bowin (1976),

$$Z(k) = \frac{C(k)}{E_t(k)} \quad \dots (3.38)$$

where, k is the wavenumber, $Z(k)$ is gravitational admittance between gravity and topography; $C(k)$ is cross spectrum of the gravity and topography, $E_t(k)$ is power spectrum of the topography and could be expressed as

$$C(k) = \frac{1}{N} \sum_{m=1}^N \Delta g_m(k) H_m^*(k) \quad \dots (3.39)$$

$$E_t(k) = \frac{1}{N} \sum_{m=1}^N H_m(k) H_m^*(k) \quad \dots (3.40)$$

Where, $\Delta g(k)$, $H(k)$ are now the Fourier transforms of the observed free-air gravity anomaly and topography, N is the number of ship tracks and the asterisk denotes the complex conjugate.

A key parameter in the admittance analysis is coherence, which gives the measure of gravity produced by seafloor topography. The coherence can be computed using the following equation (Watts, 2001)

$$\gamma^2(k) = \frac{C(k)C^*(k)}{E_g(k)E_t(k)} \quad \dots (3.41)$$

where, $E_g(k)$ the power spectrum of free-air gravity field and can be expressed as

$$E_g(k) = \frac{1}{N} \sum_{m=1}^N \Delta g_m(k) \Delta g_m^*(k) \quad \dots (3.42)$$

The coherence can be used to separate energy spectrum into two parts (Watts, 1978)

$$\text{CohrentEnergy} = \gamma^2(k) E_g(k) \quad \dots (3.43)$$

$$\text{IncohrentEnergy} = (1 - \gamma^2(k)) E_g(k) \quad \dots (3.44)$$

Coherent energy is defined as the part of the energy in the gravity signal that is caused by bathymetry, therefore the most confident determination of the admittance function can be carried out.

The admittance is complex parameter, but in general, the real part is only used for analysis. However, phase of admittance θ is also important as it is an indicator of the coherence between free-air gravity and seafloor topography. The phase in the range of high coherence is expected to be close to zero. The phase of admittance can be computed using the following equation (Louden, 1981).

$$\theta = \arctan \left[\frac{\text{Im } Z(k)}{\text{Re } Z(k)} \right] \quad \dots (3.45)$$

The plus/ minus standard deviation (σ) in the admittance is computed from the variance of the coherence estimator as (Louden, 1981)

$$\sigma = \left[\frac{(\gamma(k))^{-2} - 1}{2n} \right]^{1/2} Z^2(k) \quad \dots (3.46)$$

Where n is the number of discrete samples in the wavenumber band.

The application of admittance analysis for the study of isostatic response of the Comorin Ridge and the Ninetyeast Ridge is described in detail in Chapter-4 and Chapter-6, respectively.

3.7 Process Oriented Gravity Modeling

Process oriented gravity modeling is an extremely useful and widely accepted technique in order to investigate the geologically complex regions, where the gravity anomalies have

been changed through geological ages. Earlier Watts (1988) and Watts and Fairhead (1999) have used this technique to study the complex rifted continental margins in terms of crustal structure, subsidence history and long-term mechanical properties of the crust. In this analysis, the observed gravity anomaly was considered as a sum of several processes those were involved during the evolution of continental margins such as rifting, underplating, sediment loading, flexure, erosion, etc. The technique essentially involves 2D flexural backstripping and computation of gravity anomalies corresponding to relevant processes at the margin.

The aim of backstripping is to reconstruct the basement configuration of the basin prior to the sediment and water loading. The 2D backstripping procedure consists of flexural

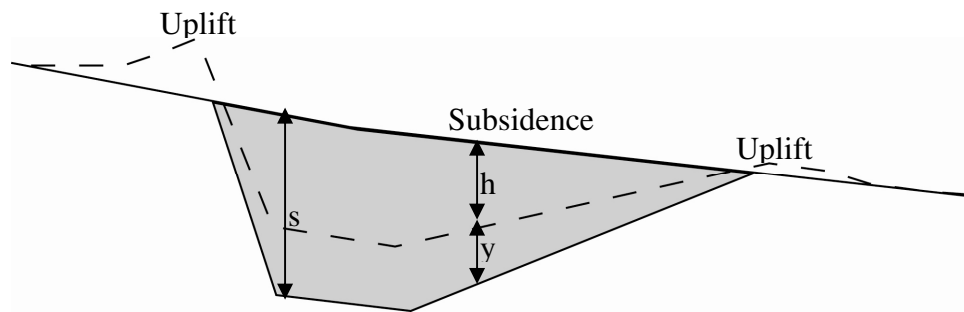


Figure 3.4 The principle of backstripping. The shaded region represents the wedge of sediments. The dashed line is backstripped basement in the absence of sediment loading.

unloading of each sedimentary layer identified from seismic section from the top downwards. The flexure of basement due to sediment loading is computed using elastic plate theory as described in section (3.5). The flexure $y(x)$ due to a sediment load of present day thickness $s(x)$ and density ρ_s (Figure 3.4) is expressed as (Watts, 2001)

$$Y(k) = \frac{-(\rho_s - \rho_w)}{(\rho_m - \rho_w)} S(k) \Phi_e(k) \quad \dots (3.47)$$

$Y(k)$, $S(k)$ are Fourier representations of $y(x)$ and $s(x)$ and $\Phi_e(k)$ is the isostatic response function. The backstrip $h(x)$ is calculated from

$$h(x) = s(x) - y(x) \quad \dots (3.48)$$

This concept of process oriented modeling is used for investigating the structure and isostatic compensation of the 85°E Ridge. The details of the method are discussed in detail in Chapter 5.

3.8 Geophysical Data

In this study, ship-borne bathymetry, gravity and magnetic profiles available in NGDC database are compiled with data collected on various Indian and Russian cruises in eastern Indian Ocean. From this database selected geophysical profiles crossing the Comorin Ridge, 85°E Ridge and Ninetyeast Ridge were used for the study in this research work.

Multichannel Seismic reflection data along with gravity and bathymetry data collected on board *MV Sagar Sandhani* (profiles MAN-01 and MAN-03), *ORV Sagar Kanya* (profile SK107-7) and *RV Issledovatel* (Profile 98791) are used for the model studies of 85°E Ridge (Chapter 5). Geophysical data acquisition were carried out using similar instruments during *MV Sagar Sandhani* and *ORV Sagar Kanya* cruises; Integrated Navigation System (Magnavox 1107) along with Global positioning System for position fixing, DFS V system for seismic data, KSS-30, 31 Bodenseewerk system for gravity data and Honeywell Elac narrow beam echosounder system for bathymetric data. Free-air gravity anomalies are computed from the acquired gravity data by applying Eotvos correction and normal gravity (GRS 67 reference ellipsoid). Seismic data processing was done at Interra Exploration Company (India) Pvt. Ltd., Bombay for profiles MAN-01 and MAN-03, at SPIC, ONGC, Mumabi for profile SK107-07 and on-board *RV Issledovatel* for profile 98791.

These data sets along with their profile locations and other details are presented in Chapters 4, 5 and 6. Additionally, satellite-derived gravity (Sandwell and Smith, 1997, 2009) and bathymetry (Smith and Sandwell, 1997; GEBCO; ETOPO) data sets are also used wherever necessary. GMT software (Wessel and Smith, 1995) is extensively used for data processing and figure preparations.